Spring 2019

Effects of Initial Thermal Structure on the Evolution of Continental Rifting

Alexandra Wernle
wernlea@cwu.edu

EFFECTS OF INITIAL THERMAL STRUCTURE ON THE EVOLUTION OF CONTINENTAL RIFTING

A Thesis

Presented to

The Graduate Faculty

Central Washington University

In Partial Fulfillment

of the Requirements for the Degree

Master of Science

Geological Sciences

---

by

Alexandra Wernlé

May 2019

CENTRAL WASHINGTON UNIVERSITY

Graduate Studies

We hereby approve the thesis of

Alexandra Wernlé

Candidate for the degree of Master of Science

APPROVED FOR THE GRADUATE FACULTY

_____ _____

Dr. Audrey Huerta, Committee Chair

_____ _____

Dr. Paul Winberry

_____ _____

Dr. Walter Szeliga

_____ _____

Dean of Graduate Studies

ABSTRACT

EFFECTS OF INITIAL THERMAL STRUCTURE ON THE EVOLUTION OF CONTINENTAL RIFTING

by

Alexandra Wernlé

May 2019

Continental rifting is a fundamental earth process that displays a wide variety of styles ranging from narrow to wide, symmetric and asymmetric, magmatic and amagmatic. The key conditions and processes that control the evolution of rifts remain enigmatic. Previous research suggests that the initial thermal structure may have a first order control on the evolving styles of these systems. This project examines the impact of the initial thermal structure on the spatial and temporal evolution of continental rifts using finite element thermo-mechanical modeling.

The initial thermal structure is a product of crustal heat production rates and heat conducted from the asthenosphere (lithospheric thickness); therefore, we explore the impact of varying crustal heat production rates from 0.75 to 2.25 $\mu w/m^3$, and lithospheric thicknesses of 100 to 200 km. The model captures continental lithospheric crust and mantle with an orogenic welt of over-thickened crust. The modeled strength, strain field, and thermal structure evolve in response to initial conditions using an iterative time-stepping algorithm. The model results display distinct styles of continental rifting.

Simulations with initially cold temperatures at the base of the orogenic crustal welt result in narrow rifts. Simulations with initially cooler temperatures at the base of the crustal

welt result in symmetric rift geometries, while simulations with initially higher basal crust temperatures deform asymmetrically. Simulations with more asthenospheric contribution to basal crust temperatures evolve as wider rifts, whereas simulations with more crustal contribution evolve as less wide rifts.

Thus, our results show that the initial thermal structure has a first-order control on the symmetry of rifting, on wide versus narrow extension styles, and the width of the rift zone. Models compare favorably to real rift systems such as the Red Sea Rift and the West Antarctic Rift System, verifying the application of the models.

ACKNOWLEDGMENTS

I would like to express my appreciation to Dr. Audrey Huerta for her constructive suggestions and dedication during the development of my thesis project. She has helped me grow into the researcher that I am today and provided me with amazing opportunities to travel and network. Audrey is a devoted advisor who is committed to the growth of her students and the quality of their research.

Assistance with Matlab programming and thesis editing provided by Dr. Paul Winberry is also greatly appreciated. He efficiently solved any programming difficulties that I encountered and also provided many original scripts for simulating the model. His help made the research process smoother.

I would like to offer my thanks to Dr. Walter Szeliga for his editing contributions to my project and his excellence as a professor in Seismology. He provided valuable suggestions and clarifications on the content of this work and furthered my understanding of a related field.

I would also like to express my gratitude towards my family, friends, and peers for supporting me through this process. They made the experience more enjoyable and were always understanding of the intense work that goes into a master's thesis.

TABLE OF CONTENTS

Chapter		Page
I.	INTRODUCTION	1
	Objectives	3
II.	BACKGROUND	4
	Styles of Rifting: Observed Geometries and Modeled Processes	4
	Insight from Models: Key Parameters Controlling Rift Evolution	7
III.	METHODOLOGY	12
	Restatement of Topic	12
	Model Explanation	12
	Parameter Testing	16
	Initial Conditions	18
IV.	RESULTS	20
	Initial Thermal Structure: Control on Rifting Style	20
	Processes Controlling Modes of Rifting	22
	Summary of Results	33
	Model Uncertainties	34
V.	COMPARISON OF MODEL RESULTS WITH RIFT SYSTEMS	35
	Examples of Modeled Rifting Styles	35
	Rift Jumping Styles	37
VI.	CONCLUSIONS	39
	REFERENCES	40
	APPENDIXES	49
	Appendix A: Initial Observations	49
	Appendix B: Example of Rift Jumping Style	51

LIST OF TABLES

Table		Page
1	Estimated Parameters for Extended Regions	9
2	Initial and Explored Parameters	16

LIST OF FIGURES

Figure		Page
1	Wide and Narrow Rifting Modes	2
2	Initial Model Setup	14
3	Two Examples of a Steady-State Geotherm	19
4	Graph of Final Rift Architecture	21
5	Example of Narrow Rifting Style Evolution	25
6	Example of Wide, Symmetric Rifting Style Evolution	28
7	Example of Wide, Asymmetric Rifting Style Evolution	31
8	Potential Rift Jumping Style	38
9	Rifting Style as a Function of Heat Production versus Spreading Rate	50
10	Evolution of the Rift Jumping Style	52

CHAPTER I

INTRODUCTION

Rifting is a large-scale tectonic process that occurs in regions where the lithosphere undergoes extensional deformation. Commonly, rifting starts in areas of weaknesses such as reactivated suture zones, or areas of thickened crust, created during plate tectonic processes (Wilson, 1966). Margins of rifted regions display significant variations in architecture, volcanism, and sedimentation, suggesting variations in the relative role of different processes or conditions in these regions.

Previous studies recognize four end-member styles of rifting: Wide and narrow rifts (England, 1983; as cited in Buck, 1991), symmetric and asymmetric rifts (Huismans and Beaumont, 2003), as well as rift systems that evolve between these styles. Classic examples of the narrow style include the East African Rift System (Ebinger et al., 1989), the Baikal Rift (Zorin, 1981), and the Rio Grande Rift (Morgan et al., 1986). The Basin and Range is an example of wide rifting (Hamilton, 1987), and the West Antarctic Rift System is an example of a system evolving from a wide to a narrow style of rifting (Huerta and Harry, 2007). For every rift system, extension always occurs in the weakest column of the lithosphere at a given time. For example, it has long been recognized that narrow rifting is characterized by a strong system in which the same location remains the weakest throughout the evolution of the rift (England, 1983; Kusznir and Park, 1987; as cited in Buck, 1991). On the other hand, wide rifting occurs in weaker systems where the locus of extension continually shifts until break-up (Figure 1). A rift system may

transition between these wide and narrow rifting styles due to changes in the evolving strength of the lithosphere. Rift systems may also be classified by their symmetry; Asymmetric rifts occur when lithospheric extension is unequally distributed along the margins, whereas symmetric rifts form with well-distributed, centralized extension. These distinct rifting styles result from the strength of the lithosphere, and because the strength of the lithosphere is dominated by the initial thermal structure (Huerta and Harry, 2007, Buck, 1991), we investigate how the initial thermal structure controls rifting style evolution.

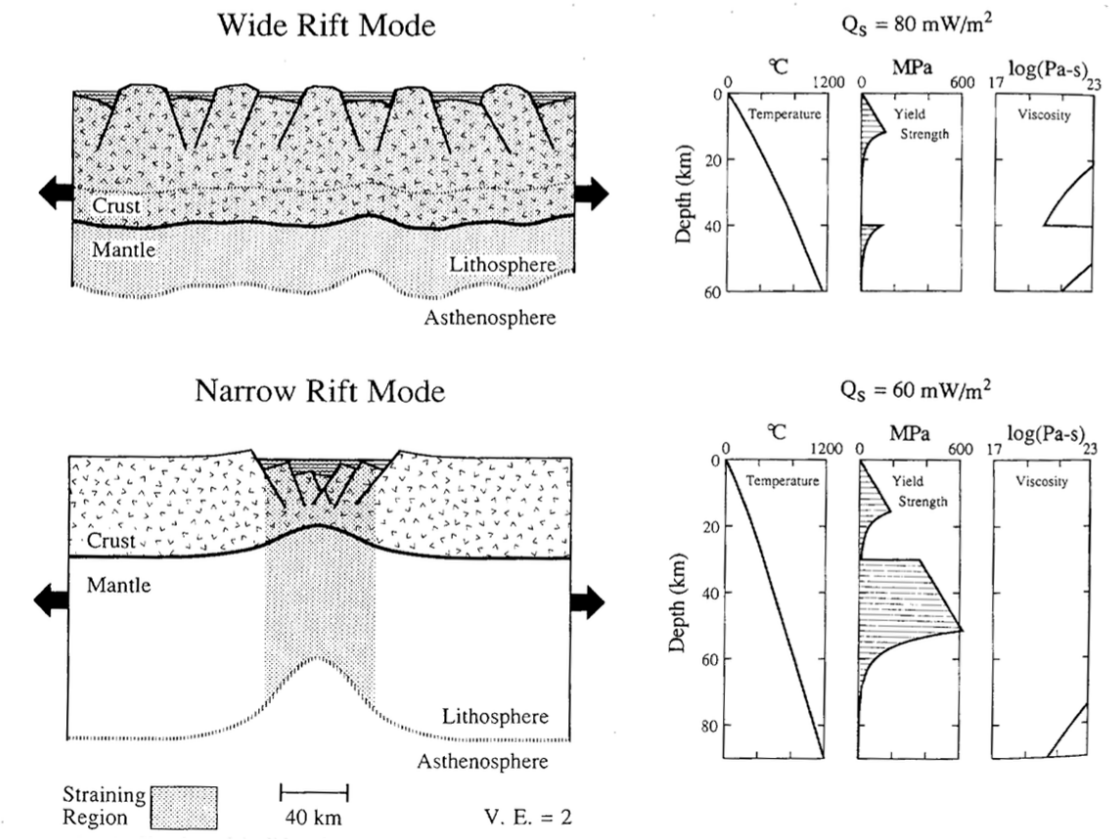

Figure 1. Wide and narrow rifting modes and their initial model geotherms, yield

strengths, and effective viscosities (Buck 1991).

Objectives

This study will use numerical modeling of continental rifting to explore the controls on the evolution of rift systems, specifically the key processes and conditions that lead to wide and narrow, symmetric and asymmetric rift modes. To accomplish this, we will use dynamic finite element thermo-mechanical modeling to simulate extension under a constrained set of initial and boundary conditions (Huerta and Harry, 2007). We find that the initial temperature at the base of the crust in the center of the orogenic welt (Tci) predicts narrow styles, symmetric and asymmetric styles, and that the source of the heat contribution controls how wide the system is.

CHAPTER II

BACKGROUND

Styles of Rifting: Observed geometries and modeled processes

Narrow Mode Rifting

Narrow rifting styles have been observed in classic examples such as the Rhinegraben, the Gulf of Suez, the Northern Red Sea, the East African Rift, the Baikal Rift, and the Rio Grande Rift (Ebinger et al., 1989; Zorin, 1981; Morgan et al., 1986). Narrow mode rifting is defined as the localization of lithospheric thinning during the rifting stage, also known as necking. Narrow rifting is characterized by a strong system in which the same location remains the weakest throughout the evolution of the rift (England, 1983; Kusznir and Park, 1987; as cited in Buck, 1991). The strength of the continental lithosphere for the narrow rift mode exhibits a strong crust and mantle with a thin section of ductile lower crust, also known as the jelly sandwich strength model (Burov and Diament, 1995; as cited in Burov and Watts, 2006).

Key modeled processes that form narrow rifts are: Mechanical weakening of the lithosphere due to thinning of the lithosphere, faults and ductile shear zones (Zuber and Parmentier, 1986; as cited in Brune et al., 2016), and rift-related melting generating dikes which also weaken the thermal and mechanical lithosphere (Buck, 2007; as cited in Brune et al., 2016). The localized thinning of the lithosphere causes the advection of heat upwards to be faster than thermal diffusion (Buck, 1999), and as a result, the thinned area

remains the weakest area, and concentrates extension (England, 1983; Kusznir and Park, 1987; as cited in Buck, 1991).

Wide Mode Rifting

Wide rifting styles are also globally observed in examples such as the Basin and Range and the Aegean Sea (Hamilton, 1987). Wide rifting is defined as a delocalized mode, or crustal thinning and extension migrates through time, and commonly occurs in orogenic regions of thicker than normal crust (Hamilton, 1987; as cited in Buck, 1991). Wide rifting occurs in weaker systems where the locus of extension continually shifts until break-up (Buck, 1991). The strength of the continental lithosphere for wide rift modes exhibits a strong crust and a uniformly weak mantle, also known as the crème-brûlée strength model (Jackson, 2002; as cited in Burov and Watts, 2006).

Modeled processes show that the thinning of the crust makes that location stronger and thus cooler, which causes the strain to migrate to another locality (Buck, 1991). This mechanism is often associated with thick crust and high heat flow, and thus an initially weak and ductile lithosphere. The ductile flow allows the thick crust to spread out, leaving cooler stronger crust (Buck, 1991).

Symmetric and Asymmetric Modes of Rifting

Symmetric and asymmetric rifts have been identified in nature; including the symmetric South China Sea and the asymmetric Tasmania Divergence Zone (TDZ) of the

East African Rift System (Clift and Lin, 2001; Franke et al., 2014; Clift et al., 2002; Lin et al., 2004; as cited in Brune et al., 2016; Ring, 2014). Symmetric and asymmetric rifting styles have been incorporated into modern terminology and are classified by the symmetry of extension during rifting (Huismans and Beaumont, 2003). We also define the symmetry of our models based on the symmetry of the extending lithosphere. For example, if the amount of crustal extension on both sides of a rift is equal, it is a symmetric rift. If one side of a rift has been hyperextended relative to the other, it is considered an asymmetric rift. Although these rifting styles characterize the symmetry of extension, the primary mode of extension is wide and therefore the same modeled processes apply. *Tetreault and Buiter's* [2018] study did find that 1) ultraslow extension rates create symmetric margins, 2) intermediate to high extension rates create crust-mantle decoupling and produce wide, asymmetric margins.

Transition from Wide to Narrow

Rifting regions may evolve between styles of rifting, for example, the transition from a wide to a narrow style of rifting has been observed in the West Antarctic Rift System. The transition between the modeled processes of a localized to a delocalized mode of rifting may be controlled by the thermal regime. *Huerta and Harry* [2007] suggest thermal weakness near rift edges is a key factor in shifting the locus of extension from wide to narrow rifts. They found that the cooling and strengthening of the

lithosphere leads to a transition from a wide mode of extension to a narrow mode of extension.

Insight from Models: Key parameters controlling rift evolution

Brief Overview

Rifting is a complex process that results from deep, dynamic crust and mantle processes that the scientific community has limited ability to geologically sample. Therefore, an optimal method for studying rifts are analogue and numerical modeling methods that enable us to explore key conditions and processes controlling rifting evolution in combination with geologic observations at rift margins.

Analogue models have been used to analyze lithospheric processes with multi-layer materials to simulate crustal thinning, isostatic adjustment, asymmetric rifts and more (Corti and Manetti 2006; Corti, 2008; Agostini et al., 2009; Autin et al., 2010,2013; Cappelletti et al., 2013; Corti et al., 2013; Nestola et al., 2013, 2015; as cited in Brune et al., 2016). However, these simplified laboratory models are not sufficient to capture the regional-scale, long-term evolution of the rheology, thermal structure and architecture of rift margins.

Numerical modeling techniques are able to account for more complex systems including the evolving thermal structure and stress-dependent viscosity. This allows numerical models to produce a more complete picture of an evolving lithosphere. Two-dimensional and more recently three-dimensional numerical modeling has become the

primary investigative tool for studying rifting processes; the following section will discuss key parameters in more detail.

Extensional Velocity

Buck [1991] looked at estimated conditions for a variety of observed narrow and wide rift systems using geologic and geophysical data (Table 1). He found no significant difference between extensional velocities for different rifting styles, except for the Aegean Sea area that is anomalously high.

Tetreault and Buiter [2018] characterized different rifting styles in their study on the effects of extensional velocities on the evolution of passive margins. They found that total extension rates for observed continental rifts range from 1-20 km/my, with slow rates in the Rio Grande Rift (.2-1.2 km/my) and fast rates in the Afar Rift (<20 km/my). They modeled the interplay between extension rates and rheology, and found that they are greatly related in passive margin evolution. Their results show: 1) ultraslow extension rates (2 km/my) create symmetric margins, 2) intermediate to high extension rates (10-50 km/my) create crust-mantle decoupling and produce wide, asymmetric margins, 3) fast extension rates (30-50 km/my) lead to narrow margins when the crust and mantle are coupled, 4) and that medium-fast (20 km/my) extension rates with ductile lower crust forms rift jumping styles.

Table 1. Estimated parameters for extended regions using geological data ((8)Eaton, 1963; (9)Lachenbruch and Sass, 1978; (10)Eddington et al., 1987; (11)Makris, 1978;

(12)Jongsma, 1974; (13)Jackson and McKenzie, 1988; (14)Morgan et al., 1985; (15)Morgan, 1982; (16) *Buck* [1991] assumes less than the total Basin and Range extension rate; (17)Makris et al., 1981; (18)Joffe and Gaffunkel, 1987; (19)Ebinger et al., 1989; (20)Iilies and Greinier, 1978; (21)Zorin, 1981; as cited in and modified from Buck, 1991).

Location	Crustal Thickness (km)	Heat Flow (mW/m^2)	Extension Velocity (cm/yr)
Wide Rifts			
North Basin and Range	25-35 (8)	90 (9)	0.8-1.1 (10)
Aegean Sea area	30-35 (11)	90 (12)	3-10 (13)
Narrow Rifts			
Rio Grande	30 (14)	60(15)	<1 (16)
Gulf of Suez	30 (17)	40 (18)	0.5-0.7(19)
Northern Red Sea	30 (17)	40 (14)	0.7-1.5 (18)
East African Rifts	40 (19)	50(15)	0.1 (19)
Rhinegraben	40 (20)	70 (15)	0.1 (20)
Baikal Rift	40 (21)	50 (15)	?

Crustal Rheology

Crustal rheology plays a crucial role on the formation in numerical models of wide versus narrow rifting (Buck, 1991). *Brune et al* [2016] used a model setup of distinct material layers based on geologic observations. They used a felsic upper crustal layer and a mafic lower crust. They found that strong, cold crust supports crust/mantle coupling and the formation of narrow rifts, and that hot, weak crust supports decoupling

between the crust/mantle boundary and the formation of wide rifts. Therefore, different rheologies can produce different rifting styles.

Sedimentation Rate

Bialas and Buck [2009] suggest that low sedimentation rates may increase the time in the wide rift mode because crustal thinning migrates from the central part of the plateau structure towards the edges. Low sedimentation rates may lead to the rift edges being starved in sedimentation while the center of thinning accumulates sediment. Therefore, the central areas of the rift can have depressed isotherms leading to cooler and stronger crust, while the zone of active rifting becomes focused at the two plateau edges that remain hot and weak. The center and edges of the thinned area in a rift plateau instead have depressed isotherms when the model transitions to narrow rifting.

Thermal Structure

Buck [1991] noted that the thermal regime plays a critical role in the mode of extension and is highly affected by the heat flow and crustal thicknesses. The estimated heat flow for wide rift modes is around 90 mW/m^2, which is significantly higher than narrow rift modes (40-70 mW/m^2) (Table 1). The estimated crustal thicknesses are also less than 50 km for both wide and narrow rift modes (Table 1).

Huerta and Harry [2007] suggest thermal weakness near rift edges is a key factor controlling the mode of extension. In their models, the lithosphere cools and strengthens

because of thinning of the upper crust and a corresponding reduction of heat being generated by the crust. Therefore, diffused/wide extension may transition to narrow extension because of cooling the upper mantle/lower crust under constant regional extension rates.

CHAPTER III

METHODOLOGY

Restatement of Topic

Since there is a growing body of literature indicating the thermal structure plays a primary role in the strength of the lithosphere and of rifting evolution, this study will focus on the impact that the initial thermal structure has on the evolution of continental rifting. Because the initial thermal structure of the lithosphere is determined by two factors (heat produced in the crust and conducted from the asthenosphere), we will focus on the effect of the crustal heat production, and the thickness of the lithospheric mantle in a simplified finite element model (Figure 2).

Model Explanation

How the Model Works

We use a two-dimensional, finite element model representing a two-layer lithosphere composed of quadrilateral elements (Figure 2). The model is originally known as Strch92, a Langrarian finite element model written using FORTRAN by Harry and Grendell (Rice University), and further developed by *Dunbar and Sawyer* [1989]; therefore, we use their discussion of methods and *Huerta and Harry* [2007] as a primary reference. The dynamic model's strength, strain field, and thermal structure evolve in response to boundary conditions using an iterative time-stepping algorithm. The algorithm first solves for the strain rate and effective viscosity using the Navier-Stokes

equation for a nonlinear visco-plastic medium. At the next time step, each element deforms according to the weaker of either a pressure dependent brittle failure criterion or by power-law ductile creep (Equations in Table 2). Elements typically deform according to the yield criterion for brittle failure at lower temperatures with high differential stress (Byerlee, 1968). Elements fail according to the criterion for ductile-creep at higher temperature conditions and deform viscously in a non-Newtonian style. Our model does not deform by discrete faulting; however, it is approximated using continuous ideal plastic deformation. Ideal plastic deformation allows slip to occur in all directions instead of the strength being limited along a fault surface. After the strain is calculated for each element, the transient heat equation is solved to account for the thermal effects of conduction, convection, and advection by solving for temperature throughout the model at the next time step. The resulting model calculates the spatial and temporal evolution of a deforming lithosphere.

Model Geometry, Initial and Boundary Conditions

The model captures a two-layer lithosphere of crust and lithospheric mantle with an orogenic welt geometry of over-thickened crust (Figure 2-Initial geometry). The non-welt portion of the crust is 30 km thick, whereas the welt is 42 km thick. The length of the modeled lithosphere is 1000 km, and the length of the crustal welt is 340 km. The initial model setup of a two-layer lithosphere begins in thermal steady-state with heat production within the crust, and boundary conditions of 0° C at the top, and

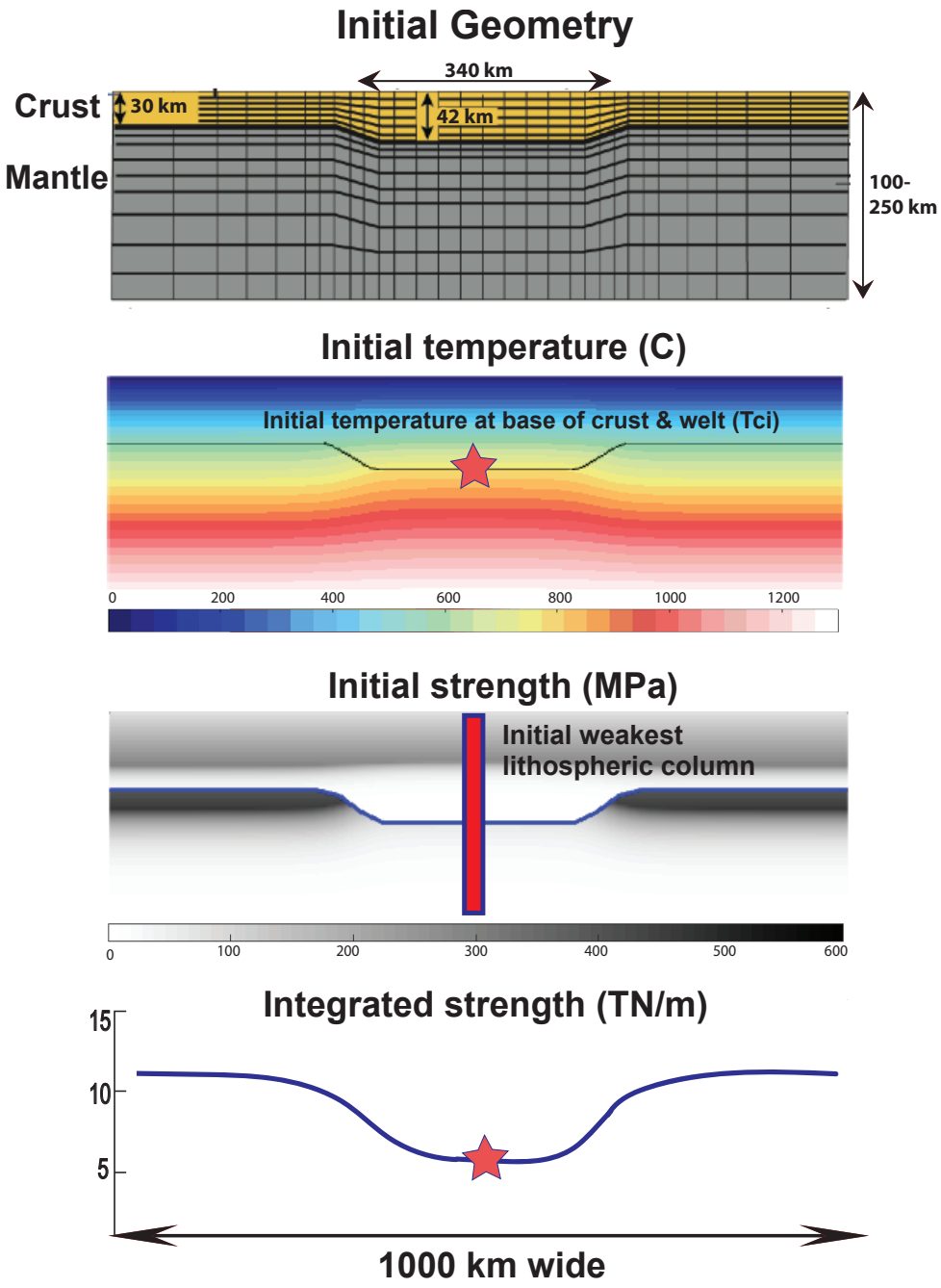

Figure 2. Initial model setup showing the initial geometry of lithosphere, the initial thermal structure, the initial mechanical structure, and the integrated strength.

1300° C at the bottom (Figure 2-Initial temperature). The 1300°C boundary condition is meant to simulate heat from the asthenosphere, assuming that a constant temperature of the asthenosphere is maintained by convectional mixing. On the sides of the model, an insulator boundary condition is applied (dt/dx = 0).

The mechanical boundary conditions of Strch92 are constant horizontal extension rates on the sides, and vertical buoyancy forces. The buoyancy forces account for lateral density variations associated with changes in composition, temperature, crustal thickness, and basin fill. Regions of the model that drop below sea level during the model simulation are water loaded.

The elemental grid is relatively coarse (800 elements); therefore more, smaller, elements are placed in regions that experience high strain. We use two material layers to represent the crust and the lithospheric mantle; the crustal rheology uses a diorite composition, while a dunite composition is applied to the lithospheric mantle (Table 2). We assume a crustal density of 2850 kg/m^3 and a mantle density of 3300 kg/m^3 (Table 2). We assume initial sea level height is level with the top of the non-welt lithosphere and that the mantle geoid height is 2.5 km less than the designated sea level. We assign a value of $1x10^{-15}$ (epsilon dot) for the initial strain rate throughout the lithosphere.

Table 2. Initial and explored (highlighted) parameters applied to the crust and mantle for the model setup. Equation for viscous rheology calculates ductile deformation and equation for plastic rheology calculates brittle deformation.

Constant and Explored (yellow) Parameters:		
Rheologic parameters		
	Crust	Mantle
Viscous rheology, equation: $\sigma = [\dot{E} / A]^{1/n} e^{Q/nRT}$		
A, $s^{-1} Pa^{-n}$	5e−18	4e−25
Q, kJ mol^{-1}	219	498
n	2.4	4.5
ρ, kg m^{-3}	2850	3300
Plastic rheology, equation: $\sigma = S+Bz$		
S, MPa	60	60
B, MPa km^{-1}	11	11
Thermal parameters		
Heat production, μW m^{-3}	.75 to 2.25	0
Thermal Conductivity, W m^{-1} °C^{-1}	2.5	3.4
Specific heat, J kg^{-1} °C^{-1}	875	1250
Coefficient of thermal expansion, °C^{-1}	3.1e−5	3.1e−5
Layer thickness		
Crust, km	30 and 42	
Lithosphere, km	100 to 250	
Velocity and strain		
Constant velocity (km/my)	10 on each side	
Strain rate	1.0e-15	

Parameter Testing

The intent of the modeling is to simulate the temporal and spatial evolution of rifting, and models with different initial thermal structures. Specifically, we change the initial thermal structure by varying two parameters:

1) Heat production rates within the crust
2) Lithospheric and crustal thicknesses

The crust is a primary heat-producing source within the lithosphere as a result of its internal radiogenic heating from the decay of elements such as Uranium, Thorium, and Potassium. Measurements of average crustal heat production tend to average around ~ 0.4-0.7 $\mu w/m^3$ (Rudnick et al., 1998; Jaupart and Maraschael, 2003; Hasterock and Chapman, 2011) with measured values as anonymously high as ~4.6 $\mu w/m^3$ in areas such as Southern Australia (McLaren et al., 2003). We will use crustal heat productions rates from as low as 0.75 $\mu w/m^3$ to as high as 2.25 $\mu w/m^3$. Heat production is distributed uniformly throughout the modeled crustal domain.

Thickness of continental lithospheres have been estimated to range from as much as 280 km to as little as 40 km using modeling of long-period surface waves (Pasyanos, 2008). The lithospheric thickness has a critical impact on the geotherm; therefore, we will investigate the impact of lithospheric thicknesses from as low as 100 km to as high as 250 km in increments of 25.

The relative role of the initial crustal heat production rates versus lithospheric thicknesses on the thermal structure can be captured by a single parameter, the initial temperature at the base of the center of the crustal welt (Tci) (Figure 3).

Initial Conditions

Our model begins in a steady state thermal structure with a constant thermal boundary condition of 1300° C at the bottom of the lithosphere, 0° C at the top of the crust, and heat produced within the crust. Thus, the initial thermal structure varies significantly depending on the initial lithosphere thickness and crustal heat production rate. Specifically, the initial geotherm in the center of the orogenic welt reflects the relative importance of the two sources of heat. Figure 3 shows two examples of initial geotherms from the center of the welt. The geotherm on the left is using a thick lithosphere and a high crustal heat production rate, while the geotherm on the right is using a thin lithosphere with a low crustal heat production rate. We can see that when using a crustal heat production rate greater than 0 (red line), the temperature at the base of the crust (Tci) increases. Therefore, the space between the blue and the red geotherm represents the crustal contribution the Tci. When using a thin lithosphere (right) versus a thick lithosphere (left), the Tci also increases. This increase is due to the asthenospheric contribution (blue arrow), which is greater when the asthenosphere is closer to the base of the crust. The Tci and the source of the heat contribution are crucial to the evolution of rifting styles.

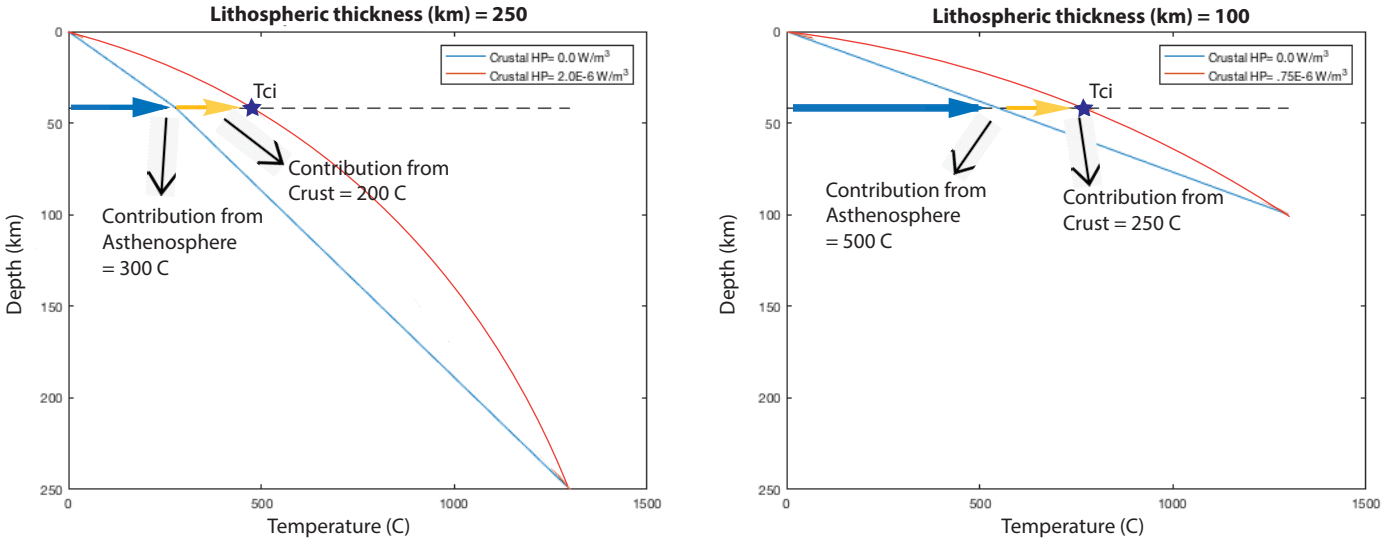

Figure 3. Figure showing two examples of a steady-state geotherm in our model. The geotherm on the left is using a thick lithosphere and a high crustal heat production rate. The geotherm on the right is using a thin lithosphere with a low crustal heat production rate. The blue line represents a geotherm based on a crustal heat production rate of 0, while the red line represents the modeled geotherm based on the crustal heat production rate.

The initial thermal structure consists of a warmer lower crust in the center of the welt (Figure 2-Initial temperature). The initial strength within the lithosphere is always weakest in the center of the welt, with a stronger upper mantle below the non-welt crust (Figure 2- Initial strength). The thick welt of the crust results in the weakest lithosphere in the center of the welt. This weakness is due to two factors:

1) Weak lower crust replaces strong upper mantle
2) Warmer and weaker crust in the welt versus the sides of the model domain

CHAPTER IV

RESULTS

Initial Thermal Structure: Control on rifting style

To explore the impact of the initial thermal structure on the rifting evolution of continental lithosphere, we varied crustal heat production rates and initial lithospheric thicknesses from 0.75 $\mu w/m^3$ to 2.25 $\mu w/m^3$ and from 100 km to 250 km. After applying a constant velocity to the sides of the model domain, the simulations were allowed to evolve until the crustal thickness reached 8 km (simulating rupture). Figure 4 shows the final lithospheric geometry of 36 model runs that result from varying the initial thermal structure. The bottom x-axis represents the asthenospheric contribution to Tci and the y-axis shows the crustal contribution to Tci. The top x-axis shows the lithospheric thicknesses associated with each asthenospheric contribution. The isopleths represent the initial temperature at the base of the crust in the center of the orogenic welt (Tci). We identify three primary styles of rifting; 1) Style 1 is narrow, 2) style 2 is wide, symmetric, and 3) style 3 is wide, asymmetric. The narrow styles are found only in regions of cool Tci (~<700° C), whereas wider styles are found at hotter Tci (~>700° C). The symmetric styles are consistently located in relatively cool Tci (~<750-800° C) and asymmetric is always located in regions with higher Tci (~>750° C).

The source of heat contribution to the Tci has a primary control on the final widths of wide (symmetric, and asymmetric) rifting styles. Simulations with higher

asthenospheric contribution to the Tci result in a wider rifting geometry, while higher crustal contribution to the Tci result in a less wide rifting geometry.

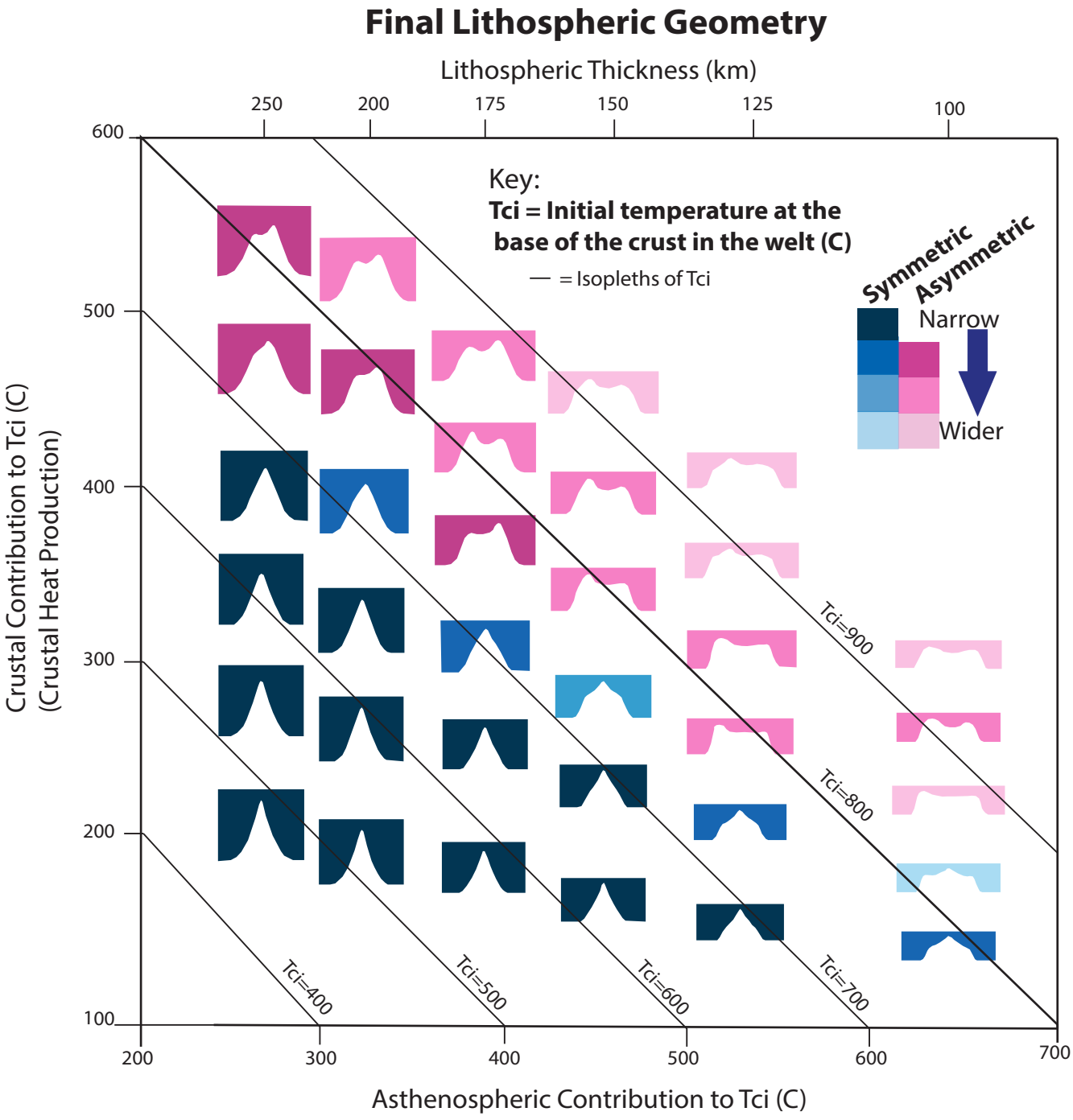

Figure 4. Final rift architecture as a function of crustal contribution (crustal heat production rates) and asthenospheric contribution (lithospheric thickness) to the temperature at the base of crust. Bold isopleths represent boundaries for initial temperature at the base of the crust in the center of the orogenic welt (Tci). Crustal heat productions rates increase in the y-direction and are constant for each row of model runs. Lithospheric thicknesses are displayed on the top x-axis and are constant for each column of model runs.

Processes Controlling Modes of Rifting

To further understand the mechanisms controlling rift style, we investigate the evolution of the simulations focusing on the thermal structure and strength. Figures 5, 6, and 7 show the evolution of the three modeled rifting styles identified in Figure 4; 1) Style 1 is narrow, 2) style 2 is wide, symmetric, and 3) style 3 is wide, asymmetric. The displayed evolution of each style proceeds from initial to final conditions of the whole lithosphere and the details of the weakest column (where failure occurs) at key time steps. To further explore the impact of the evolving thermal structure, we track the temperature at the base of the crust of the weakest lithospheric column (Tc). We analyze the evolution in terms of the thermal structure, the geotherm at the weakest column, the lithospheric strength profile, the integrated strength profile, and the strength profile at the weakest lithospheric column (starred). The lithospheric strength profile shows the shear

strength and is calculated using Byerlee's Law (Byerlee, 1968). The integrated strength profile is calculated by integrating the shear strength within each lithospheric column.

Example of Narrow Rifting Style

Figure 5 shows an example of our modeled narrow rifting style. At time 0 m.y. (Figure 5A), the initially thick lithosphere has a relatively cool thermal structure with a cool Tci of ~480° C. The strength profile shows that the cooler lithosphere produces a very strong crust and upper mantle, with only a thin layer of weak, ductile crust in the crustal welt. The integrated strength at the center of the crustal welt is ~37 TN/m. The strength profile at the weakest lithospheric column shows a jelly-sandwich model (Burov and Diament, 1995; as cited in Burov and Watts, 2006) with a weak ductile lower crust between a strong upper crust and upper mantle.

From timesteps 7 to 11 m.y. (Figure 5B and C), the thick lithosphere continues to thin at the same, initially weak location at the center of the welt. As the lithosphere extends, the temperature at the base of the crust (Tc) decreases (~460° C), and the thin lithosphere weakens, with the integrated strength at the center of the welt reduced to ~18-8.8 TN/m. The strength at the weakest lithospheric column shows weakening due to thinning, and less strong crust and upper mantle with more significant weakening of the upper mantle than the crust.

By 15 m.y. (Figure 5D), rupture occurs in the same, initially weak lithospheric column. The Tc decreases to ~400° C, and the integrated strength at the center of the

crustal welt drops to ~2.5 TN/m. The strength profile at the weakest lithospheric column shows the loss of ductile lower crust, and the upper mantle and crust become completely coupled.

Overall, narrow rifting proceeds by continued failure of the central lithospheric column, which remains the weakest column of the lithosphere. The crust and upper mantle weaken as the lithosphere extends and the Tc decreases until they become completely coupled at rupture.

Example of Narrow Rifting Style

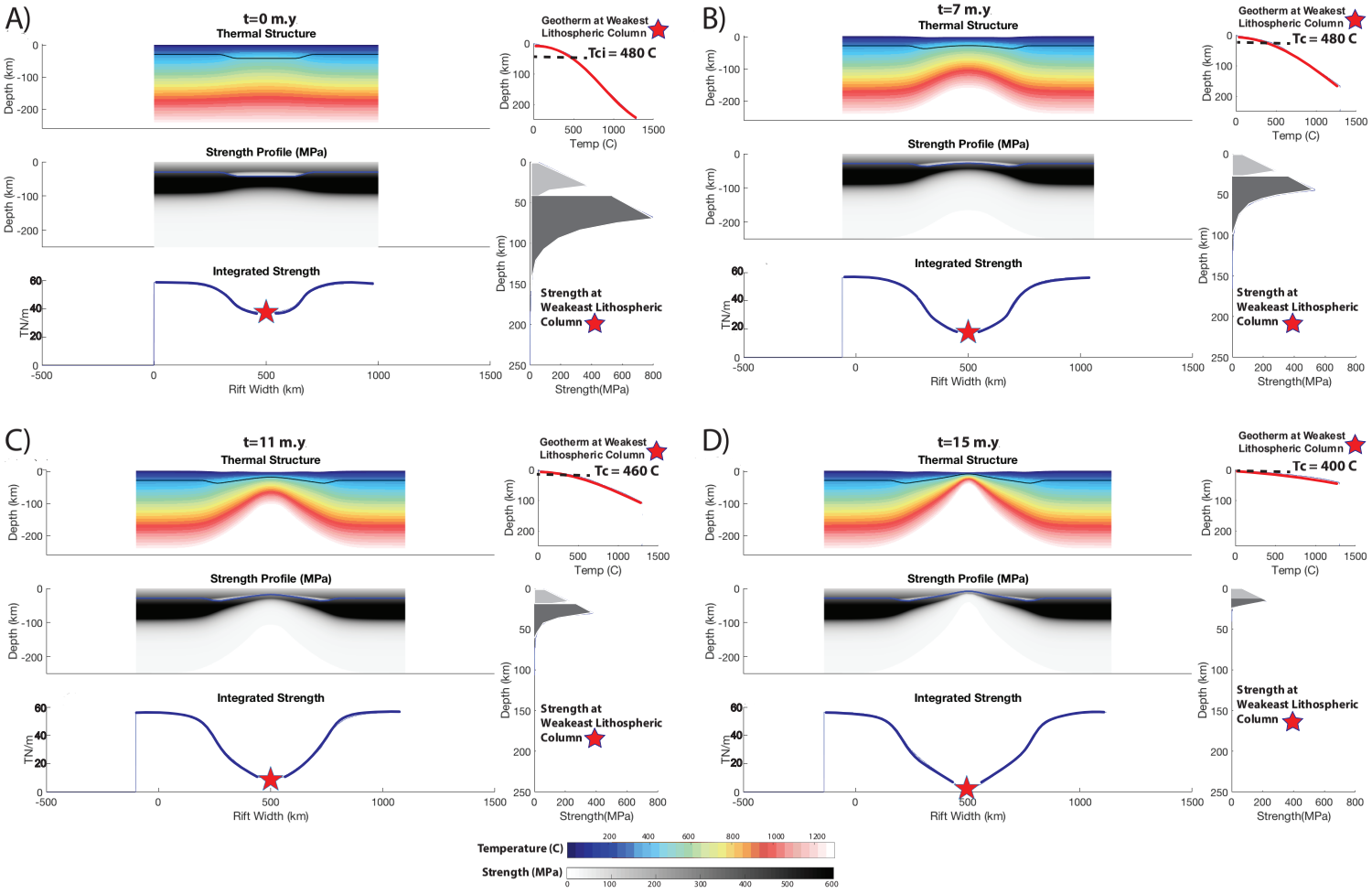

Figure 5. Figure showing the evolution of the narrow rifting style identified in Figure 4. The evolution proceeds from initial to final conditions in terms of the thermal structure, the geotherm, the integrated strength profile, the lithospheric strength profile, and the strength profile at the weakest lithospheric column. The star on the integrated strength profile indicates the location of the weakest lithospheric column, and also where the geotherm and the strength at the weakest lithospheric column profiles are sampled. The Tci (and Tc) show the temperature at the base of the crust in the center of the crustal welt at the weakest lithospheric column.

Example of Wide, Symmetric Rifting Style

Figure 6 shows an example of our modeled wide, symmetric rifting style. At time 0 m.y. (Figure 6A), the initially thin lithosphere has a hot thermal structure with a warmer Tci of ~820° C. The strength profile shows that the hotter lithosphere produces a weak lower crust and mantle, with a 20 km thick layer of ductile crust in the crustal welt. The integrated strength at the center of the crustal welt is ~3.2 TN/m, which is significantly weak compared to the narrow rifting style. The strength profile at the weakest lithospheric profile shows a crème-brulee strength model (Jackson, 2002; as cited in Burov and Watts, 2006) with a decoupled, strong upper crust, a thick and ductile lower crust, and a very weak mantle.

At 9 m.y. (Figure 6B), the thinned lithosphere extends in a diffuse manner with the weakest lithospheric column now located right of the center at the base of the crustal

welt. The temperature at the base of the crust of this column (Tc) has decreased (~790° C). The thinned lithosphere now has an integrated strength at the weakest column of ~1.9 TN/m. The strength at the weakest lithospheric column shows a slight weakening of the crust, a thinning of the ductile lower crust, and a strengthening of the upper mantle.

From times 10 to 15 m.y. (Figure 6C), the thin lithosphere extends in a diffuse manner and the weakest lithospheric column progressively shifts from the margins of the crustal welt towards the center of the crustal welt. The Tc slightly decreases in temperature (~780-740° C) and the integrated strength remains constant (~1.8 TN/m) but the weakness extends towards the margins of the crustal welt. The strength at the weakest lithospheric columns shows a slight weakening of the crust and more strengthening of the upper mantle due to cooling.

By 28 m.y. (Figure 6D), rupture occurs in the center of the crustal welt. The lithosphere now displays a focused mode of rifting with a cooler Tc (~650° C) and an integrated strength of ~.99 TN/m at the center of the welt in the crust. The strength profile at the weakest lithospheric column shows that the lower ductile crust has thinned out, and the upper mantle has weakened.

Overall, the wide, symmetric rifting style initially extends by diffuse deformation and then transitions to a focused weakening in the center of the model. As the Tc decreases and the lithosphere continually thins, the ductile lower crust flows in a diffuse, decoupled style. With continued crustal thinning, the upper mantle cools and initially strengthens then weakens at rupture, and the ductile crust thins out resulting in a final

focused mode of rifting.

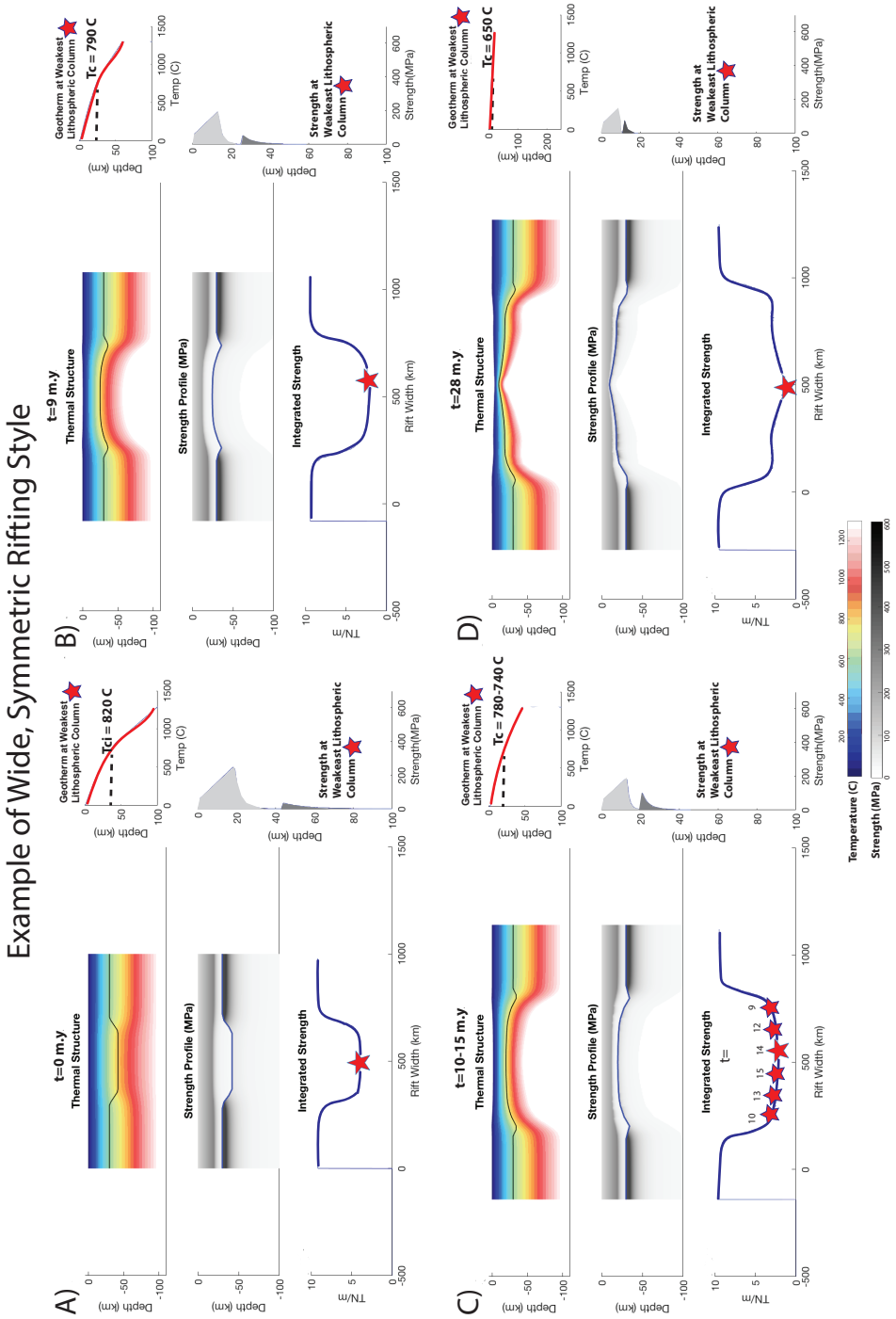

Figure 6. Figure showing the evolution of the wide, symmetric rifting style identified in Figure 4. The evolution proceeds from initial to final conditions in terms of the thermal structure, the geotherm, the integrated strength profile, the lithospheric strength profile, and the strength profile at the weakest lithospheric column. The star on the integrated strength profile indicates the location of the weakest lithospheric column, and also where the geotherm and the strength at the weakest lithospheric column profiles are sampled. The Tci (and Tc) show the temperature at the base of the crust in the center of the crustal welt at the weakest lithospheric column.

Example of Wide, Asymmetric Rifting Style

Figure 7 shows an example of our modeled wide, asymmetric rifting style. At time 0 m.y. (Figure 7A), the initially thin lithosphere has a hot thermal structure with a hotter Tci of ~870° C. The strength profile shows that the hotter lithosphere produces a weak lower crust and mantle with a ~22 km thick ductile lower crust in the welt. The integrated strength at the center of the crustal welt is ~2.7 TN/m, which is weaker than the wide, symmetric style of rifting. The strength profile at the weakest lithospheric column shows a crème-brulee strength model (Jackson, 2002; as cited in Burov and Watts, 2006) with a strong upper crust, a thick and ductile lower crust, and a very weak mantle.

At times 10 to 20 m.y. (Figure 7B), the thinned lithosphere extends in a diffuse manner and the weakest lithospheric column progressively shifts from the margins towards the center of the crustal welt. As the crustal welt thins, the temperature at the

base of the crust (Tc) decreases (~820- 730° C) and the integrated strength drops to ~1.7 TN/m across the crustal welt. The strength at the weakest lithospheric column shows a slight weakening of the upper crust, thinning of the ductile lower crust, and strengthening of the upper mantle.

At times 20 to 25 m.y. (Figure 7C), the thinned lithosphere continues to extend in a diffuse manner and the weakest lithospheric column progressively shifts from the center of the crustal welt towards the margins of the crustal welt. The Tc does not show a significant decrease in temperature (~730- 690° C) and the integrated strength remains constant across the crustal welt. The strength at the weakest lithospheric columns shows the same strength in the upper crust, the ductile lower crust, and the upper mantle.

By 34 m.y. (Figure 7D), rupture occurs on the margin of the crustal welt. The lithosphere now displays a focused mode of rifting with a relatively cooler (but still hot) Tc (~670° C) and an integrated strength of ~.91 TN/m at the margin of the crustal welt. The strength at the weakest lithospheric column shows that the upper mantle and crust have both weakened, and the ductile lower crust has thinned.

Overall, the wide, asymmetric rifting style initially extends by diffuse deformation and then transitions to a focused thinning on the margins of the model. As the Tc decreases and the lithosphere continually extends, the ductile lower crust flows in a diffuse, decoupled style. With continued crustal thinning, the upper mantle cools and initially strengthens, then weakens at rupture. The warmer margins of the crustal welt (~670° C) cause the margins to become weaker than the center of the crustal welt.

As extension continues, thinning focuses on the margins of the crustal welt instead of the center. The result is a final focused mode of rifting on the margins of the crustal welt.

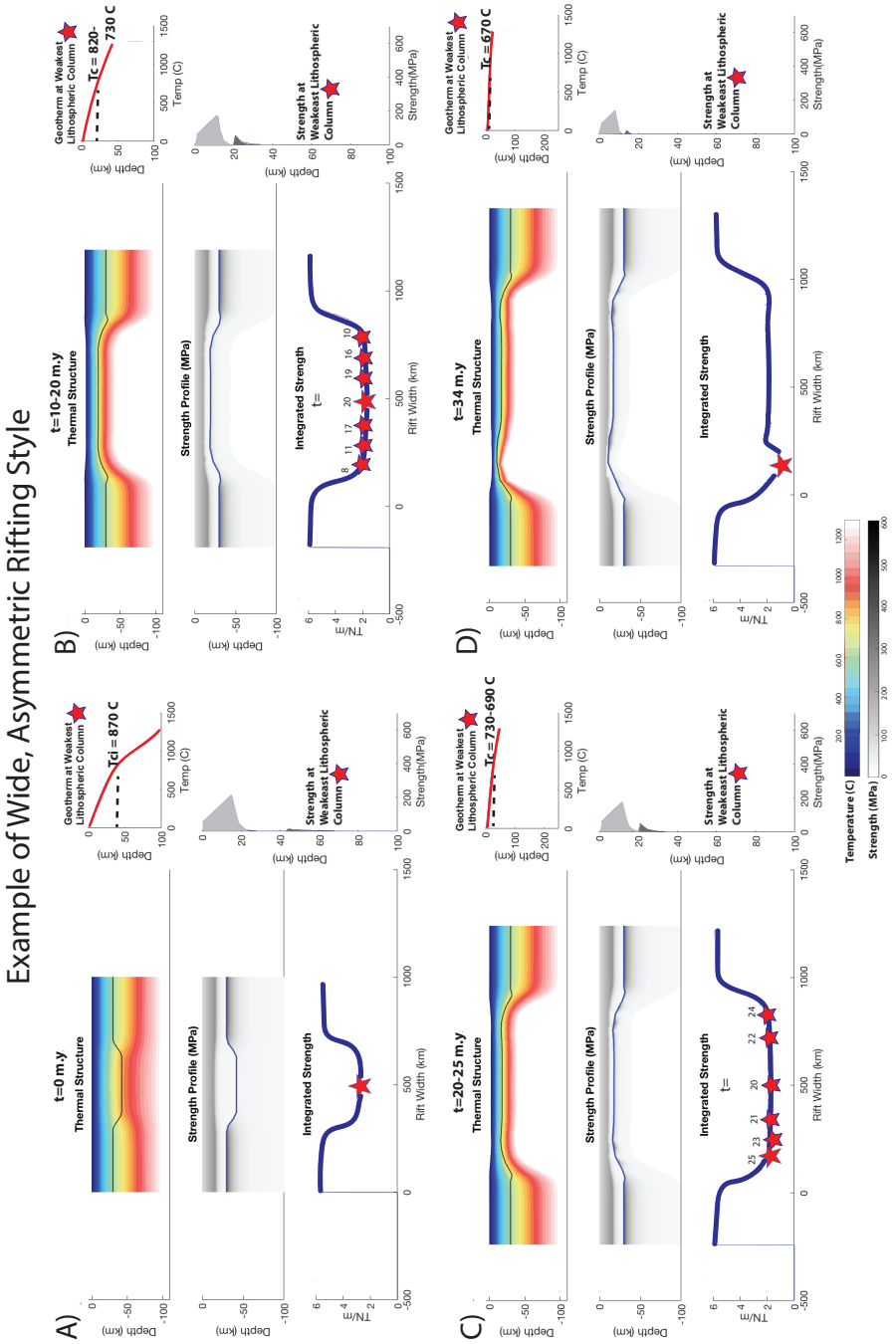

Figure 7. Figure showing the evolution of the wide, asymmetric rifting style identified in Figure 4. The evolution proceeds from initial to final conditions in terms of the thermal structure, the geotherm, the integrated strength profile, the lithospheric strength profile, and the strength profile at the weakest lithospheric column. The star on the integrated strength profile indicates the location of the weakest lithospheric column, and also where the geotherm and the strength at the weakest lithospheric column profiles are sampled. The Tci (and Tc) show the temperature at the base of the crust in the center of the crustal welt at the weakest lithospheric column.

Key Points

Our analysis of strength evolution shows that narrow rifting proceeds by failure of the central lithospheric column, which remains the weakest column of the lithosphere. For narrow modes of rifting, as the lithosphere thins and the asthenosphere upwells, the lithosphere thermally weakens due to thinning and the proximity of the hot asthenosphere (Buck et al., 1999; Kuznir and Park, 1987; as cited in Svartman Dias et al., 2015). For wide modes of rifting, we find that lithospheric thinning causes the upper mantle to initially strengthen due to cooling, and then weaken at rupture. We also find that colder lithospheric structures have a thinner ductile lower crust that leads to localized deformation, whereas hotter lithospheric structures have a decoupled crust and mantle that allow for lower crustal flow, cooling and strengthening of the upper mantle, and a wider mode of extension

Summary of Results

The patterns we identify in the control of the initial thermal structure on the evolution of rifting styles show:

1) Cooler initial basal crust temperatures (~<700° C) form narrow styles

2) Higher (~>700° C) basal crust temperatures result in wider rifting styles

3) Cooler initial basal crust temperatures (~<750°-800° C) result in symmetric rifting styles

4) Higher basal crust temperatures (~>750° C) form asymmetric rifting styles

Simulations with more asthenospheric contribution to basal crust temperatures evolve as weak, wider rifts, whereas simulations with more crustal contribution evolve as strong, less wide rifts.

We identify three major styles of rifting; 1) Style 1 is narrow, 2) style 2 is wide, symmetric, and 3) style 3 is wide, asymmetric. The example of a narrow rifting style displays a constant, centralized location of necking, in which the middle column is always the weakest. The example of a wide, symmetric rifting style displays a transition from a diffused mode of weakening to a focused weakening in the center of the model. The example of a wide, asymmetric rifting style displays a transition from a diffused mode of weakening to a focused weakening on the margins of the model.

Model Uncertainties

Our two-dimensional model presents a simplified version of a continental rift system and is not meant to simulate every possible parameter. Our model assumes a simple two-layer lithospheric rheology, a constant extensional velocity, and uniform crustal heat production. We also do not produce finer features such as faults or dikes. These minimal assumptions inherently present many uncertainties in relation to the real world. However, our goal was to create an overall model of continental rifting styles that develop based on initial thermal structure, not to capture the complexity of a specific extensional system. For the purpose of our study, simplicity and efficiency is preferred.

CHAPTER V

COMPARISON OF MODEL RESULTS WITH RIFT SYSTEMS

Examples of modeled rifting styles

Many end-member models exist for rift systems, however observed rift systems are often complicated and may deform by different styles along the length of the rift. Here we will briefly discuss global comparisons of continental rifts and other extensional systems to our key modeled rifting styles and a special case

Narrow Style

Narrow continental rifting styles have been globally identified in classic examples such as the Rhinegraben, the Gulf of Suez, the Northern Red Sea, the East African Rift, the Baikal Rift, and the Rio Grande Rift (Ebinger et al., 1989; Zorin, 1981; Morgan et al., 1986; as cited in Buck 1991). For example, the Red Sea Rift is an example of the narrow rifting style. *Ligi et al.* [2011] conducted a study on the Red Sea Rift using aerial magnetic and seismic reflection data, geochemical analysis and mantle flow modeling. They theorized that focused asthenospheric upwelling in the Red Sea Rift was driven by contact with thick and cold lithosphere because of a strong horizontal thermal gradient. Their findings are consistent with our model results that predict narrow rifting in cold lithospheres.

Wide, Symmetric Style

Examples of rifted margins with overall symmetry include the South China Sea, and the mid Norway margin (Brune et al., 2016; Péron-Pinvidic et al., 2013; as cited in Tetreault and Buiter, 2018. The South China Sea has wide margins and is a primarily symmetric passive margin (Brune et al., 2016). Rift-related sediments show evidence of rapid extension within the basin due to the very weak and warm thermal conditions of the crust (Clift and Lin, 2001; Franke et al., 2014; Clift et al., 2002; Lin et al., 2004; as cited in Brune et al., 2016). Seismic data indicates a possible initial crustal thickness of 33 km and a relatively thin initial lithospheric thickness of around 120 km (Nissen et al., 1995b; Artemieva, 2006; as cited in Brune et al., 2016). The geometry and associated warm thermal structure of the South China Sea is consistent with our model results that predict wide rifting in relatively warm lithosphere.

Wide, Asymmetric Style

Wide, Asymmetric extensional systems have been commonly identified in nature. Classic examples include the Aegean Sea, the West Antarctic Rift System, the Tasmania Divergence Zone, the Iberia-Newfoundland conjugates, and the Central South Atlantic (Hamilton, 1987; as cited in Buck, 1991; Huerta and Harry, 2007; Ring, 2014; Brune et al., 2016).

The West Antarctic Rift System (WARS) originated with wide extension and transitioned to narrow rifting near the Victoria Land Basin (Busetti, 1999). This transition

from a wide to a narrow mode of extension would be associated with warm lithosphere, either from high crustal heat production and/or high heat flux from the asthenosphere. Recent tomographic results display low velocity zones beneath portions of the region, suggesting high asthenospheric heat flow (White-Gaynor et al., 2019). Our model results indicate the WARS is exemplified in our wide, asymmetric rifting style in which the margin cools and strengthens, producing coupling of the crust and mantle.

Rift Jumping Style

Tetreault and Buiter [2018] characterized the rift jumping style in their modeling study on the effects of extensional velocities on the evolution of passive margins. They find that the rift jumping style occurs with intermediate extension rates and thick ductile crustal layers, where the rift jumps between the margins of the region, re-creating strong isolated crustal blocks in the center. Our model of rifting styles may also show the rift jumping style as a subset of the wide, asymmetric style (Figure 8). We also utilize intermediate extension rates with a thick section of ductile crust, where the locus of weakness continuously shifts around a crustal block. *Tetreault and Buiter* [2018] suggest that this rifting style creates an isolated continental fragment similar to H-blocks found across the North Atlantic margins (Péron-Pinvidic and Manatschal, 2010, as cited in Tetreault and Buiter, 2018). Other than passive margins, it is difficult to identify continental rift systems exhibiting this type of rifting style.

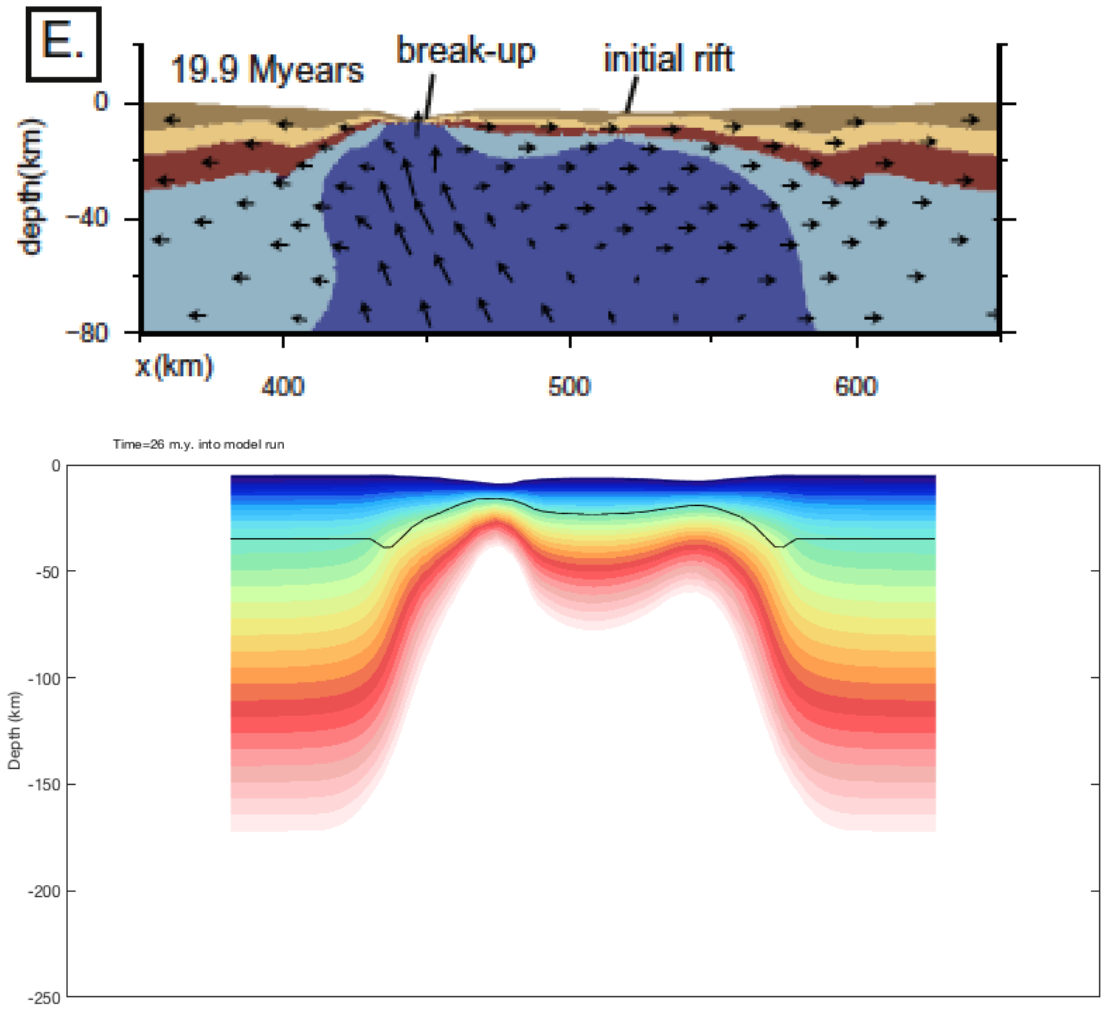

Figure 8. Comparison of our potential rift jumping style found at a crustal contribution of 420 C and an asthenospheric contribution of 390 C, to the rift jumping style of *Tetreault and Buiter* [2018].

CHAPTER VI

CONCLUSIONS

The initial thermal structure of an incipient continental rift has a first order control on the evolving and final architecture of rift margins. This project examined the spatial and temporal evolution of continental rifts using finite element thermo-mechanical modeling. We recognize that the initial thermal structure predicts three major styles of rifting; 1) Narrow, 2) wide, symmetric, and 3) wide, asymmetric.

We find that simulations with initially cold temperatures at the base of the crustal welt result in narrow rifts. Simulations with initially cool basal crust temperatures result in symmetric rift geometries, while simulations with initially higher basal crust temperatures deform asymmetrically. Simulations with more asthenospheric contribution to basal crust temperatures evolve as weak, wider rifts, whereas simulations with more crustal contribution evolve as weak, but less wide rifts.

Our two-dimensional model presents a simplified version of a continental rift system and is not meant to simulate every possible parameter similar to modern studies. These minimal assumptions inherently present uncertainties in relation to the real world. However, our goal was to create an overall model of continental rifting styles that develop based on initial thermal structure, not to capture the complexity of a specific extensional system. We hope that our research serves as a useful, simple model to aid other researchers in easily identifying big-picture similarities, for “all models are wrong, but some models are useful”- George E.P. Box.

REFERENCES

Adams, A., Miller, J., and Accardo, N., 2018, Relationships between lithospheric structures and rifting in the East African Rift System: A Rayleigh wave tomography study: Geochemistry, Geophysics, Geosystems, v.19, p. 3793– 3810: https://doi.org/10.1029/2018GC007750.

Agostini, A., Corti, G., Zeoli, A., Mulugeta, G., 2009, Evolution, pattern, and partitioning of deformation during oblique continental rifting: inferences from lithospheric-scale centrifuge models: Geochemistry, Geophysics, Geosystems, v.10, p. Q11015: http://dx.doi.org/10.1029/2009GC002676.

Artemieva, I.M., 2006a, Global 1°×°1 thermal model TC1 for the continental lithosphere: implications for lithosphere secular evolution: Tectonophysics, v. 416 (1–4), p. 245–277: http://dx.doi.org/10.1016/j.tecto.2005.11.022.

Artemieva, I.M., 2006b, Global 1°×°1 thermal model TC1 for the continental lithosphere: implications for lithosphere secular evolution: Tectonophysics, v. 416 (1–4), p. 245–277: http://dx.doi.org/10.1016/j.tecto.2005.11.022.

Autin, J., Bellahsen, N., Husson, L., Beslier, M.O., Leroy, S., d'Acremont, E., 2010, Analog models of oblique rifting in a cold lithosphere: Tectonics, v. 29, p. TC6016: http://dx.doi.org/10.1029/2010TC002671.

Autin, J., Bellahsen, N., Leroy, S., Husson, L., Beslier, M.O., d'Acremont, E., 2013, The role of structural inheritance in oblique rifting: insights from analogue models and application to the Gulf of Aden: Tectonophysics, v. 607, p. 51–64: http://dx.doi.org/10.1016/j.tecto.2013.05.041.

Bialas, R. W., and Buck W. R., 2009, How sediment promotes narrow rifting: Application to the Gulf of California, Tectonics, v. 28, p. 11,029–11,046, doi: 10.1029/2008TC002394.

Bialas, R. W., Buck, W. R., Studinger, M., and Fitzgerald, P. G., 2007, Plateau collapse model for the Transantarctic Mountains,West Antarctic Rift System: insights from numerical experiments: Geology, v. 35 (8), p. 687–690.

Brune, S., Heine, C., Clift, P.D. and Pérez-Gussinyé, M., 2016, Rifted margin architecture and crustal rheology: Reviewing Iberia-Newfoundland, Central South Atlantic, and South China Sea: Marine and Petroleum Geology, v.79, p. 257–281, doi: 10.1016/j.marpetgeo.2016.10.018.

Brune, S., 2016, Rifts and rifted margins: A review of geodynamic processes and natural hazards: Plate Boundaries and Natural Hazards (eds. J. C. Duarte and W. P. Schellart), p. 13–39, doi: 10.1002/9781119054146.ch2.

Brune, S., Heine, C., Pérez-Gussinyé, M., Sobolev, S.V., 2014, Rift migration explains continental margin asymmetry and crustal hyper-extension: Nature Communications, v.5, doi: 10.1038/ncomms5014.

Buck, W. R., Lavier, L.L., Poliakov, A.N.B., 1999, How to make a rift wide: Philosophical Transactions of The Royal Society B: Biological Sciences, v. 357, p. 671–693. doi: 10.1098/rsta.1999.0348.

Buck, W. R., 1991, Modes of continental lithospheric extension: Journal of Geophysical Research, v. 96 (20), p. 161-178, doi: 10.1029/91JB01485.

Buck, W.R., 2007, Dynamic Processes in Extensional and Compressional Settings: The Dynamics of Continental Breakup and Extension: In Treatise on Geophysics, v. 6, Crust and Lithosphere Dynamics, p. 335-376, doi: 10.1016/B978-044452748-6/00110-3.

Busetti, M., Spadini, G., van der Wateren, F.M., Cloetingh, S.A.P.L., Zanolla, C., 1999, Kinematic modelling of the West Antarctic Rift system, Ross Sea, Antarctica: Global and Planetary Change, v. 23 (1–4), p. 79–103.

Byerlee, J.D., 1968, Brittle-Ductile Transition in Rocks: Journal of Geophysical Research, v. 73 (14), p. 4741–4750.

Cappelletti, A., Tsikalas, F., Nestola, Y., Cavozzi, C., Argnani, A., Meda, M., Salvi, F., 2013, Impact of lithospheric heterogeneities on continental rifting evolution: constraints from analogue modelling on South Atlantic margins: Tectonophysics: http://dx.doi.org/10.1016/j.tecto.2013.09.026.

Clift, P., and Lin, J., 2001, Preferential mantle lithospheric extension under the South China margin: Marine and Petroleum Geology, v. 18 (8), p. 929–945: http://dx.doi.org/10.1016/S0264-8172(01)00037-X.

Clift, P., Lin, J., Barckhausen, U., 2002, Evidence of low flexural rigidity and low viscosity lower continental crust during continental break-up in the South China Sea: Marine and Petroleum Geology, v. 19 (8), p. 951–970: http://dx.doi.org/10.1016/S02648172(02)00108-3.

Corti, G., and Manetti, P., 2006, Asymmetric rifts due to asymmetric Mohos: An experimental approach: Earth and Planetary Science Letters, v. 245, p. 315–329: https://doi.org/10.1016/j.epsl.2006.02.004.

Corti, G., 2008, Control of rift obliquity on the evolution and segmentation of the main Ethiopian rift: Nature Geoscience, v. 1 (4), p. 258–262: http://dx.doi.org/10.1038/ngeo160.

Corti, G., Iandelli, I., Cerca, M., 2013, Experimental modeling of rifting at craton margins: Geosphere, v. 9 (1), p. 138–154: http://dx.doi.org/10.1130/GES00863.1.

DeMets, C., Gordon, R.G., Argus., D.F., 2010, Geologically current plate motions: Geophysical Journal International, v. 181, p. 1–80: https://doi.org/10.1111/j.1365-246X.2009.04491.x.

Dunbar, J.A., Sawyer, D.S., 1989, How preexisting weaknesses control the style of continental breakup: Journal of Geophysical Research, B, Solid Earth and Planets, v. 94, p. 7278–7292.

Eaton, J. P., 1963, Crustal structure from San Francisco, California to Eureka, Nevada from Seismic Refraction Measurements: Journal of Geophysical Research, v. 68 (20), p. 5789-5806.

Ebinger, C. J., Deino, A. L., Drake, R. E., and Tesha, A. L., 1989, Chronology of Volcanism and Rift Basin Propagation: Rungwe Volcanic Province, East Africa: Journal of Geophysical Research, v. 94, p. 15,585- 15,803.

Eddington, P. K., Smith, R. B., and Renggli, C., 1987, Kinematics of Basin and Range intraplate extension: In Continental Extensional Tectonics, edited by M.P. Coward, J. F. Dewey, and P.L. Hancock, Geological Society, London, Special Publications, v. 28, p. 371-392.

England, P. C., 1983, Constraints on extension of continental lithosphere: Journal of Geophysical Research, v. 88, p. 1145-1152.

Foster, A., & Jackson, J., 1998, Source parameters of large African earthquakes: Implications for crustal rheology and regional kinematics: Geophysical Journal International, v. 134 (2), p. 422–448: https://doi.org/10.1046/j.1365-246x.1998.00568.x.

Franke, D., Savva, D., Pubellier, M., Steuer, S., Mouly, B., Auxietre, J.L., Meresse,F., and Chamot-Rooke, N., 2014, The final rifting evolution in the South China Sea: Marine and Petroleum Geology, v. 58 (Part B), p. 704–720: http://dx.doi.org/10.1016/j.marpetgeo.2013.11.020

Hamilton, W., 1987, Crustal extension in the Basin and Range Province, southwestern United States: Geological Society, London, Special Publications, v. 28, p. 155-176.

Hasterok, D., Chapman, D.S., 2011, Heat production and geotherms for the continental lithosphere: Earth and Planetary Science Letters, v. 307, p. 59–70.

Huerta, A. D., and Harry, D. L., 2007, The transition from diffuse to focused extension: Modeled evolution of the West Antarctic Rift system: Earth and Planetary Science Letters, v. 255 (1-2), p. 133–147.

Huismans, R.S., Beaumont, C., 2003, Symmetric and asymmetric lithospheric extension: relative effects of frictional-plastic and viscous strain softening: Journal of Geophysical Research: Solid Earth, v. 108 (B10), p. 2496: http://dx.doi.org/10.1029/2002JB002026.

Illies, J. H., and Greiner, G., 1978, Rhinegraben and the Alpine system: GSA Bulletin, v. 89, p. 770-782.

Jackson, J., and McKenzie, D.P., 1988, The relationship between plate motions and seismic moment tensors, and the rates of deformation in the Mediterranean and Middle East: Geophysical Journal International, v. 93 (1), p. 45-73.

Jaupart, C., Mareschal, J.C., 2003, Constraints on crustal heat production from heat flow data: Treatise on Geochemistry, v. 3, p. 65–84, doi: 10.1016/B0-08-043751-6/03017-6.

Joffe, S., and Gaffunkel, Z., 1987, Plate kinematics of the circum Red Sea-- A re-evaluation: Tectonophysics, v. 141 (1-3), p. 5-22.

Jongsma, D., 1974, Heat flow in the Aegean Sea: Geophysical Journal International, v. 37 (3), p. 337-346: https://doi.org/10.1111/j.1365-246X.1974.tb04087.x.

Keranen, K., Klemperer, S. L., Julia, J., Lawrence, J. L., and Nyblade, A., 2009, Low lower-crustal velocity across Ethiopia: Is the Main Ethiopian Rift a narrow rift in a hot craton?: Geochemistry, Geophysics, Geosystems, v. 10 (5), doi:10.1029/2008GC002293.

Kusznir, N. J., and Park, R. G., 1987, The extensional strength of the continental lithosphere: Its dependence on geothermal gradient, and crustal composition and thickness: Geological Society, London, Special Publications, v. 28 (1), p. 35– 52, doi: 10.1144/GSL.SP.1987.028.01.04.

Lachenbruch, A. H. and Sass, J.H., 1978, Models of an extending lithosphere and heat flow in the Basin and Range province, in Cenozoic Tectonics and Regional Geophysics of the Western Cordillera, edited by R. B. Smith and G.P. Eaton: The Geological Society of America, v. 152, p. 209-250, doi: https://doi.org/10.1130/MEM152.

Ligi, M., Bonatti, E., Bortoluzzi, G., Cipriani, A., Cocchi, L., Caratori Tontini, F., Carminati, E., Ottolini, L., and Schettino, A., 2012, Birth of an ocean in the Red Sea: Initial pangs: Geochemistry, Geophysics, Geosystems, v. 13 (8), p. Q08009, doi:10.1029/2012GC004155.

Lin, J., Zhang, J., Jiang, S., Wang, S., Xu, B., and Wei, M., 2004, The neogene foraminiferal stratigraphy of the LH-19-4-1 bore hole: Pearl River Mouth Basin, South China sea: Journal of Stratigraphy, v. 28 (2), p. 120–125.

Lindenfeld, M., and Rümpker, G., 2011, Detection of mantle earthquakes beneath the East African Rift: Geophysical Journal International, v. 186 (1), p. 1–5: https://doi.org/10.1111/j.1365-246X.2011.05048.x.

Lister, G.S., Etheridge, M.A., Symonds, P.A., 1991, Detachment models for the formation of passive continental margins: Tectonics, v. 10 (5), p. 1038–1064.

Makris, J., 1978, The crust and upper mantle of the Aegean region from deep seismic soundings: Tectonophysics, v. 46 (3-4), p. 269-284: https://doi.org/10.1016/0040-1951(78)90207-X.

Makris, J., Allem, B. A., and Moller, L., 1981, Deep seismic studies in Egypt and their interpretation (abstract), EOS Trans. AGU, v. 62, p. 230.

McLaren, S., Sandiford, M., Hand, M., Neumann, N., Wyborn, L., Bastrakova, I., Hillis, R., Muller, D., 2003, The hot southern continent: heat flow and heat production in Australian Proterozoic terranes: Geological Society of Australia, v. 22, p. 151–161.

Morgan, P., 1982, Heat flow in rift zones: in Continental and Oceanic Rifts, edited by G. Palmason, Geodynamics Series, AGU, Washington, D.C., v. 8, p. 107-122.

Morgan, P., Boulos, F. K., Hennin, S. F., El-Sheriff, A. A., E1- Sayed, A. A., Basta, N. Z., and Melek, Y. S., 1985, Heat flow in Eastern Egypt: The thermal signature of a continental breakup: Journal of Geodynamics, v. 4 (1-4), p. 107-131.

Morgan, P., Seager, W. R., and Golombek, M.P., 1986, Cenozoic thermal, mechanical and tectonic evolution of the Rio Grande Rift: Journal of Geophysical Research, v. 91, p. 6263-6276: https://doi.org/10.1029/JB091iB06p06263.

Mulibo, G. D., and Nyblade, A. A., 2016, The seismotectonics of southeastern Tanzania: Implications for the propagation of the eastern branch of the east African rift: Tectonophysics, v. 674, p. 20–30: https://doi.org/10.1016/j.tecto.2016.02.009.

Nestola, Y., Storti, F., Bedogni, E., Cavozzi, C., 2013, Shape evolution and finite de-formation pattern in analog experiments of lithosphere necking: Geophysical Research Letters, v. 40 (19), p. 5052–5057: http://dx.doi.org/10.1002/grl.50978.

Nestola, Y., Storti, F., Cavozzi, C., 2015, Strain rate-dependent lithosphere rifting and necking

architectures in analog experiments: Journal of Geophysical Research: Solid Earth, v. 120 (1), p. 584–594, http://dx.doi.org/10.1002/2014JB011623.

Nissen, S.S., Hayes, D.E., Buhl, P., Diebold, J., Bochu, Y., Zeng, W., Chen, Y., 1995b, Deep penetration seismic soundings across the northern margin of the South China Sea: Journal of Geophysical Research: Solid Earth, v. 100 (B11), p. 22407–22433: http://dx.doi.org/10.1029/95JB01866.

Pasyanos, M.E., 2008, Lithospheric thickness modeled from long-period surface wave dispersion: Tectonophysics, v. 481, p. 38–50.

Péron-Pinvidic, G., Manatschal, G., 2010, From microcontinents to extensional allochthons: witnesses of how continents rift and break apart?: Petroleum Geoscience, v. 16 (3), p. 189–197: http://dx.doi.org/10.1144/1354-079309-903.

Péron-Pinvidic, G., Manatschal, G., Osmundsen, P.T., 2013, Structural comparison of archetypal Atlantic rifted margins: a review of observations and concepts: Marine and Petroleum Geology, v. 43, p. 21–47: http://www.sciencedirect.com/science/article/pii/S0264817213000287.

Ring, U., 2014, The East African Rift System: Austrian Journal of Earth Sciences, v. 107 (1), p. 132–146.

Rudnick, R., McDonough, W., O'Connell, R., 1998, Thermal structure, thickness and composition of continental lithosphere: Chemical Geology, v. 145, p. 395–411.

Simon, N. S. C., Podladchikov, Y.Y., 2008, The Effect of Mantle Composition on Density in the Extending Lithosphere: Earth and Planetary Science Letters, v. 272, p. 148–157.

Svartman Dias, A. E., Lavier, L. L., Hayman, N. W., 2015, Conjugate rifted margins width and asymmetry: The interplay between lithospheric strength and thermomechanical processes: Journal of Geophysical Research: Solid Earth, v. 120, p. 8672– 8700: doi: 10.1002/2015JB012074.

Tetreault, J.L., and Buiter, S.J.H., 2018, The influence of extension rate and crustal rheology on the evolution of passive margins from rifting to break-up: Tectonophysics, v. 746, p. 155–172: https://doi.org/10.1016/j.tecto.2017.08.029

Tommasi, A., and Vauchez, A., 2001, Continental rifting parallel to ancient collisional belts: An effect of the mechanical anisotropy of the lithospheric mantle: Earth and Planetary Science Letters, v. 185, p. 199–210, doi: 10.1016/S0012-821X(00)00350-2.

White-Gaynor, A.L., Nyblade, A.A., Aster, R., Wiens, D.A., Bromirski, P.D., Gerstoft, P., Stephen, R.A., Hansen, S.E., Wilson, T., Dalziel, I.W., Huerta, A., Winberry, J.P., and Anandakrishnan, S., 2019, Heterogeneous upper mantle structure beneath the Ross Sea Embayment and Marie Byrd Land, West Antarctica, revealed by P-wave tomography: Earth and Planetary Science Letters, v. 513. p. 40-50, doi: 10.1016/j.epsl.2019.02.013.

Wilson, J. T., 1966, Did the Atlantic Close and then Re-Open?: Nature, v. 211(5050), p. 676–681, doi:10.1038/211676a0.

Yang, Z., and Chen, W.P., 2010, Earthquakes along the East African Rift System: A multiscale, system-wide perspective: Journal of Geophysical Research, v. 115 (B12), p. 309: https://doi.org/10.1029/2009JB006779.

Zorin, Yu. A., 1981, The Baikal Rift: An example of the intrusion of asthenospherie material into the lithosphere as the cause of the disruption of lithospheric plates: Tectonophysics, v. 73, p. 91-104.

Zuber, M.T., and Parmentier, E.M., 1986. Lithospheric necking: a dynamic model for rift morphology: Earth and Planetary Science Letters, v. 77 (3–4), p. 373–383: http://dx.doi.org/10.1016/0012-821X(86)90147-0.

APPENDIXES

APPENDIX A

Initial Observations

Initial, exploratory simulations captured the impact of varying crustal heat production rates from .25 to 1.75 $\mu w/m^3$ Figure 7). Figure 7 shows a shift from a narrow rifting style to a wider rifting style as crustal heat production increases. As crustal heat production increases from 1.0 to ~1.5 $\mu w/m^{3,}$ the style transitions from symmetric to asymmetric. However, spreading velocity does not significantly impact rifting style and therefore was not used as a key parameter in later simulations.

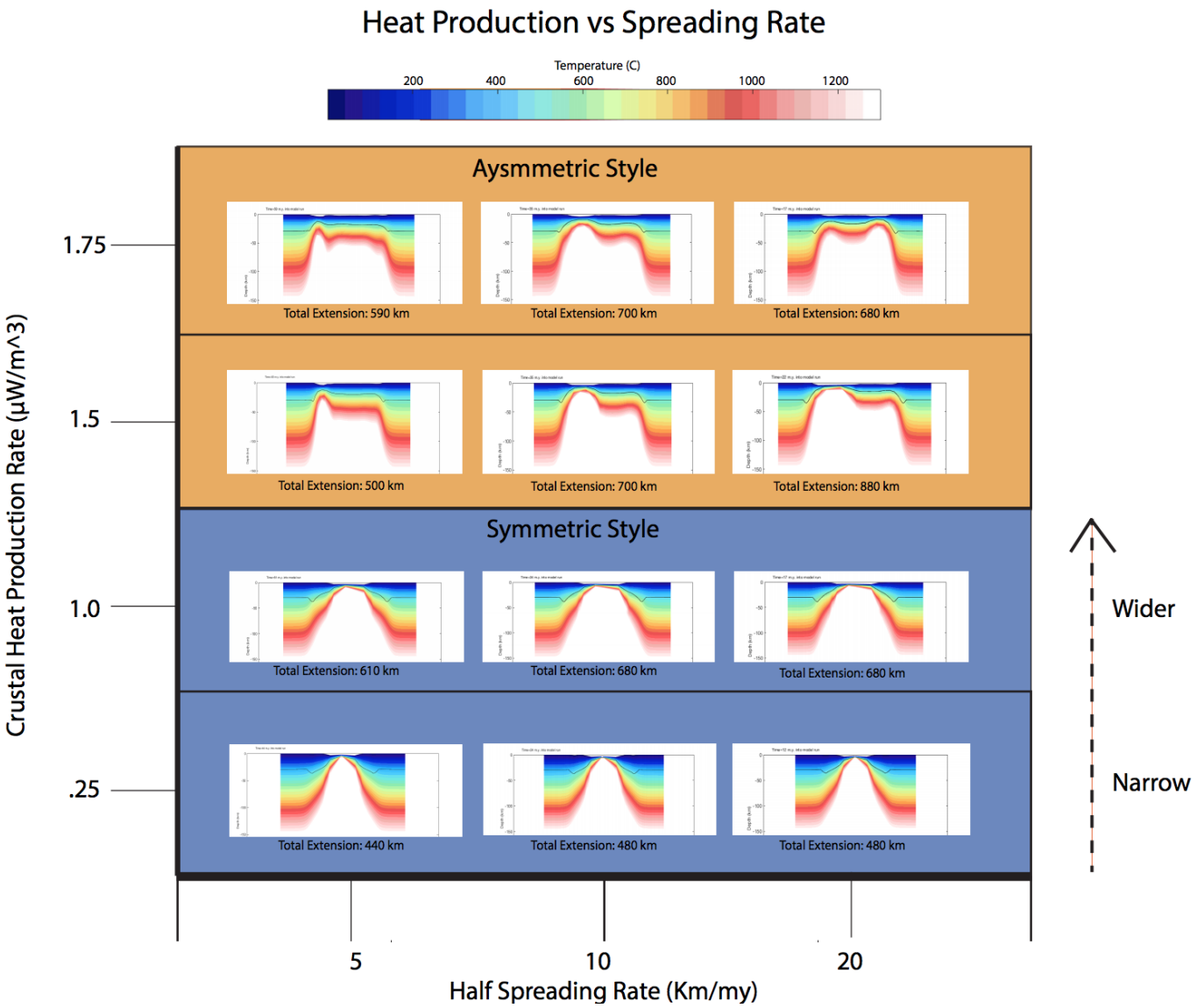

Figure 9. Graph showing rifting style as a function of heat production versus spreading rate.

APPENDIX B

Example of Rift Jumping Style

Figure 10 shows an example of a variation of our wide, asymmetric rifting style similar to the rift jumping style identified by *Tetreault and Buiter* [2018]. The rift jumping style initiates with a diffuse mode of extension that leads to focusing along the margins of the crustal welt. This creates an isolated, strong crustal block in the center of the welt. The intermediate lithospheric thickness and very high crustal heat production results in a strong upper crust with a very weak lower crust and mantle. The initial strength profile is similar to a crème-brulee model. The center of the crustal welt cools and strengthens while the margins of the crustal welt become thermally weaker. Coupling develops on the margins of the crustal welt causing the focal point of weakening to jump between both margins of the crustal welt until focusing occurs on one side of the rift.

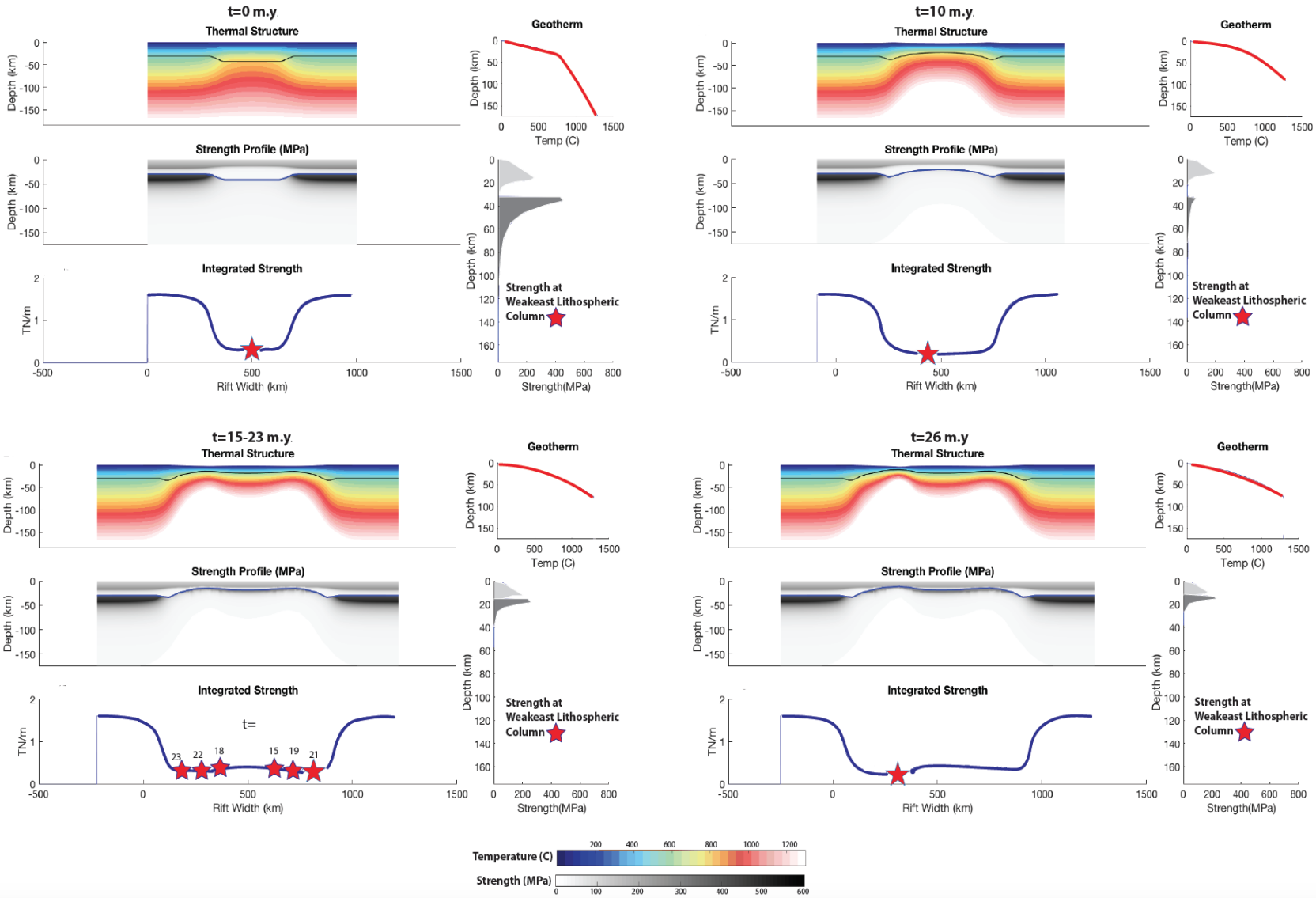
t=0 m.y
Thermal Structure
Depth (km)
Geotherm
Temp (C)
Strength Profile (MPa)
Integrated Strength
TN/m
Rift Width (km)
Strength at Weakeast Lithospheric Column
Strength(MPa)
t=10 m.y
t=15-23 m.y
t=
23
22
18
15
19
21
t=26 m.y
Temperature (C)
Strength (MPa)

Figure 10. Figure showing the evolution of the rift jumping style identified by *Tetreault and Buiter* [2018]. The evolution proceeds from initial to final conditions in terms of the thermal structure, the geotherm, the integrated strength profile, the lithospheric strength profile, and the strength profile at the weakest lithospheric column.